Automatic Segmentation of Three Dimensional Brain Magnetic Resonance Images Using Both Local and Non-Local Neighbors with Considering Inner and Outer Class Data Distances

Omid Jamshidi[1], Abdol Hamid Pilevar[1*]

1. Medical Intelligence Laboratory, Computer Engineering Department, Bu Ali Sina University, Hamedan, Iran.

Received: February 25 2014
Accepted: May 17 2014

Keywords:
Magnetic Resonance Imaging (MRI),
Segmentation,
Genetics Algorithm,
Fuzzy logic.

ABSTRACT

In this article a new combined method from genetic and fuzzy c-means algorithm (FCM) for discovering the correct number of segments and automatic segmentation of human normal and abnormal brain MR images is proposed.

For reducing the effect of the noise in segmentation process, we use the local and non-local neighbors, and also a new method for finding the appropriate neighbors of the voxels and adjusting their weights. In addition, by decreasing the distance between the data and data cluster centers, the distances between the data from other cluster centers are increased and caused a better and more precise detection of segments boundaries.

The proposed method was applied to 10 clinical MRI data set images. Our experimental results shows that the presented method has a significant improvement compare to other similar methods.

1. Introduction

Image segmentation is a complicated issue in image processing for accurate diagnosis of border between segments. In 3D image segmentation, the same label is assigned to the voxels of an image with the same visual characteristics. Some tasks such as identifying objects, feature extraction, identifying the position of objects and classification are based on their quality of image segmentation. The medical image segmentation methods can be classified into region-based [1], edge-based [2] and a combination of region and edge-based methods [3]. The purpose of medical image segmentation is to provide more meaningful images that are easier to understand and analyze. In [4], Image segmentation is carried out according to the information of edges. Some methods are using Atlas for segmentation [5, 6]. K-means and FCM can be mentioned as two region-based methods [7]. Complexity and time-consuming process of manual image segmentation for many experts necessitates the use of an automatic method. Among the methods of segmentation, FCM is more popular. The widespread use of this method is due to its simplicity and high accuracy. Due to the weaknesses of FCM in noisy image method, a few parameters have been added to it and improvement is made in it. In [8] the divisions have been carried out by the FCM objective function and the use of voxels and the neighboring voxels of any of them. In [9-11] FCM Method for changing the membership function and improving the accuracy of the segmentation is used. In [12, 13], the segmentation is done by using the objective function which is defined in FCM, non-local and local data. In [14-16], some new classification methods for calculating the weights of local points are introduced. An alternate of the FCM meth-

**** Corresponding Author:***
Abdol Hamid Pilevar, PhD
Medical Intelligence Laboratory, Computer Engineering Department, Bu Ali Sina University, Hamedan, Iran
Tel: +98 811 822 6313
E-mail: pilevar@basu.ac.ir, pilevar@gmail.com

od is used to improve the segmentation [17]. In [18], the class centers are guessed by utilizing a new algorithm based on histogram and pre-defined windows. In another study done by Lai et al. [19], a hierarchical genetic method is used. The genetic method and learning-vector quantization (LVQ) network hierarchically method for the classification of MR images is used in article [20]. In [21], a combination of pulse coupled neural network (PCNN) and statistical expectation maximization (EM) for segmentation of MR images is used. A genetic algorithm and objective function for the calculating the distance of each point from the cluster centers is used [22]. An automatic method for segmenting the cerebrospinal fluid and spinal cord from magnetic resonance images is implemented in [23].

This article proposes a new method for finding appropriate neighbors of each voxels and adjusting weights of the voxels. In each step of the algorithm we discover some more proper global neighbors for the voxels and also their related weights are calculated by using the local neighbors. The global neighbors are found and the weights of the global neighbors are adjusted simultaneously, based on FCM method. We use the genetic algorithm for classifying and segmenting the images, without having any problems such as searching for the number of segments.

2. Methods

To minimize the effect of noise on the segmentation process of the medical images, different methods based on the neighbors have been implemented. Several methods based on local neighbors and highest similarity of a voxel to its adjacent neighbors has been presented. Due to the nature of the images in medical imaging, it may happen that some voxels with more similarity are found in the areas other than adjacent voxels.

The brain image can be split into two left and right mirror section, in this two symmetric sections, the voxels of a section has a mirror voxels in the other section such that, they are similar to each other one by one, we consider these mirror voxels as good neighboring candidates for reducing the effects of the noise.

This means that, by using the local and non-local neighbors, we can achieve to better results. In this article, for an accurate segmentation, the non-local neighbors have also been used to improve the image segmentation, but it has been attempted to select the voxels from those parts of the image which by nature seems to be more similar to that voxel. Therefore, for each voxel of gray matter area of the brain, the neighbor is selected from the gray matter area. For this reason, we use matrix U generated by the FCM method.

Matrix U is a two dimensional matrix that U_ij is the degree of membership of voxel i in the data cluster j. An example of matrix U has been shown as follows:

$$U=\begin{bmatrix} 0.1 & 0.4 & 0.7 & & 0.2 \\ 0.5 & 0.3 & 0.1 & \cdots & 0.4 \\ 0.2 & 0.1 & 0.1 & & 0.1 \\ 0.2 & 0.2 & 0.1 & & 0.3 \end{bmatrix}$$

In this matrix, number of columns must be as the number of image voxels, where for example: U_{32} show that the degree of membership of the voxel 2 in data cluster 3 is 0.1.

The number of neighbors with the same class is constant. The weights of the voxel neighbors indicate the amount of their similarities to the voxel and calculated as follows.

In the first step, for each voxel, we determined the class of the 26 adjacent neighbors, by looking at matrix U. For example: in the following matrix U, there are 7 rows which mean that the number of classes is 7, and they are classified based on the highest value in each row (depicted in bold color). An illustration for a 2-D matrix is shown in Fig. 1.

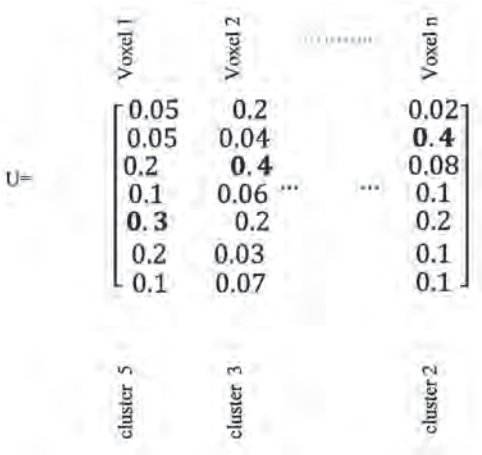

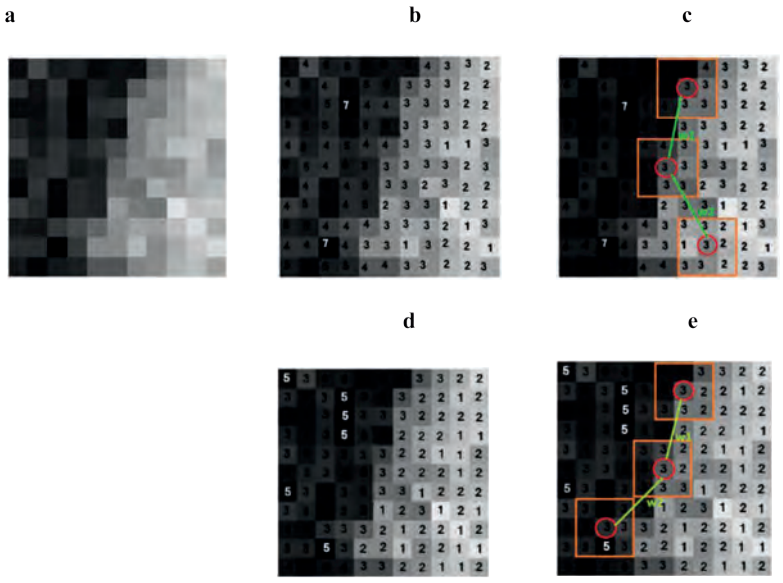

Figure 1. (a) is an unlabeled figure. (b) If matrix U has seven rows, voxels can be classified according to this matrix as shown in figure. (c) According to the area around each neighbor, we define w1 and w2. (d) If in the next step of program the chromosomes have five valid data as centers, the matrix of grey levels data can be classified as shown in figure. (e) According to the area around each neighbor, we define w1 and w2.

We compare each of the 26 neighbors of a voxel with 26 neighbors of other voxels, the neighbors are selected, according to the class that has been classified. If two voxels are classified in the same class, it means that they are considered as equal voxels. In other words, all of the 26 adjacent neighbors of each voxel are compared with all of the 26 adjacent neighbors of the other voxels that are selected as neighbors. The adjacent voxels are classified in the same class, and known as similar voxels. The number of neighbors that are classified in the same class is divided by 26 that show the effect of the selected voxel.

By using the genetic algorithm and variable number of centers in each chromosome, and with respect to the matrix U by which these centers are created, we can conclude that the number of rows of matrix U can be differ and accordingly in each step the neighbors of each voxel can be classified into different number of classes. Therefore, when matrix U has 8 rows, neighbors of each voxel can be classified between 1 and 8. We have implemented the algorithm for several times and in each run we have achieved to a better answers as discussed below.

The genetic algorithm is used and in each state more appropriate centers are identified. This means that the segments at each stage are estimated more accurately than the previous stage. Considering the fact that the neighbors for each voxels are selected from the segment in which the voxel is located. The classification of the 26 adjacent neighbors of a voxel is used to determine the weight of each voxel. In each step, with respect to the fact that the centers are estimated more accurately, the classification of the 26 neighbors of each voxel will be more correctly specified (see Fig. 2 for a 2-D illustration).

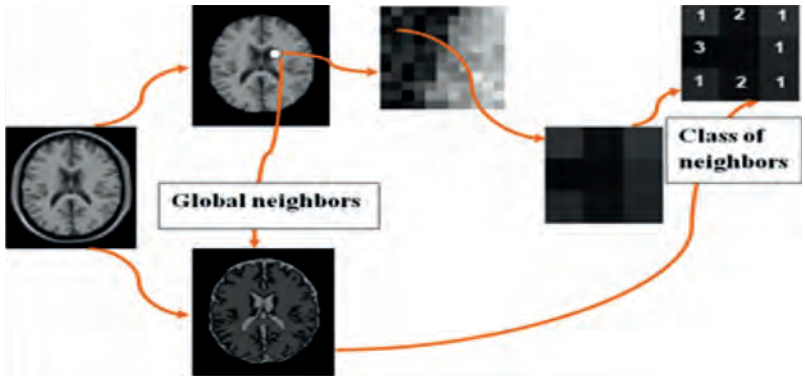

Figure 2. The schematic view.

2.1. Chromosome Representation

The centers of data are represented by chromosome values. Therefore the length of chromosome determines the number of segments in an image. The number of the data sets is controlled by the length of chromosomes, where the ranges of chromosomes are limited between 0 and 255, and the numbers are generated randomly. An example of a randomly generated chromosome has been illustrated as follows:

5.2	20.7	42	92.8	120	198

If the range of the chromosome is set to a value between 0 and 255, then it means that the length of the chromosome is the same as the number of segments. In this article we attempt to assign the number of segments automatically. Some genes of chromosome should have negative values to show that the genes are not valid as centers. The genes with negative values cannot be selected as data centers. Accordingly, the number of non-negative data in a chromosome are determined the number of data centers. Some examples of chromosomes with length of 6 are depicted in Fig. 3.

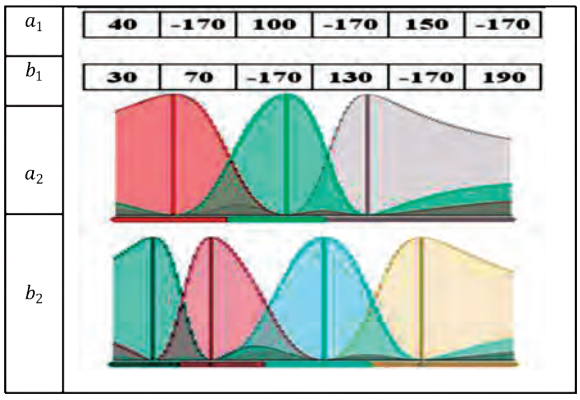

Figure 3. a1 and b1 are two chromosomes of the initial population that generated randomly and a2 and b2 are function members of a1 and b1 on random numbers.

The first chromosome shows three valid centers with the values of 40, 100 and 150. The second chromosome shows four valid centers.

2. 2. Initial Population

The initial population is constructed as follows. The number of chromosomes is initialized randomly. For some allele of the chromosomes, the negative values are assigned. The number of valid data in each chromosome can be differed. The value of chromosome alleles is changed to negative values. The minimum number of valid data on a chromosome is 2. A maximum allele can be equal to the total length of the chromosome. It should be observed that the allele may not be less than 2 valid data.

2. 3. Fitness Computation

For calculating the fitness, the FCM method is used. After data center prediction, for each chromosome, and the voxel values of the image, we complete matrix u to save membership value for each voxel. The U matrix elements will be completed according to the Formula1.

$$u_{ij} = \frac{1}{\sum_{k=1}^{c} \left(\frac{\|x_i - c_j\|}{\|x_i - c_k\|} \right)^{\frac{2}{m-1}}} \quad (1)$$

This matrix is constructed based on the inner class distances. This means that, in this process each voxel belongs to one center, in order to have the shortest distance between the data and that center. The second parameter that we want to add to FCM method is outer class consideration. This means that voxels that belong to one center have the longest distance from other centers and shortest distance from that center. We are going to change the FCM method based on these two parameters. For editing the membership of each voxel, instead of the amount of the distance of that voxel from each center, we subtract the distance of the center from 255. So, another membership function is used for the outer class distance. The objective function of inner class for matrix U is defined as Formula 2.

$$J_m = \sum_{i=1}^{N} \sum_{j=1}^{C} \sum_{n \in N_i} w_{in} u_{ij}^m \|x_i - c_j\|^2, 1 \le m < \infty \quad (2)$$

Where the value of m is greater than 1, and u_{ij} is the membership degree of x_i in the cluster j, x_i is the ith member of d-dimensional measured data, c_j is the d-dimension center of the cluster, ||*|| is the similarity between the measured data and the center,c_j is the set of centers that are stored in chromosomes, and N_i is the neighbors around voxel i.

The distance of each voxel from the center of the class equals to= 255-$(x_i$-$c_k)$

It is necessary to modify the Formula 1 to Formula 3 in the case of using the outer class data, by replacing the distance of each voxel with the center of the class.

$$u_{ij}=\frac{1}{\sum_{k=1}^{c}\left(\frac{\left\|255-(x_i-c_j)\right\|}{\left\|255-(x_i-c_k)\right\|}\right)^{\frac{2}{m-1}}} \quad (3)$$

The J_m in Formula 2, refers to U matrix and related to the inner class data, we show it as f1, and another J_m that refers to U matrix and related to inner class is shown as f2. By combining these two parameters the amount of fitness is determined by Formula 4.

$$Fitness = \alpha \times f_1 + (1-\alpha) \times f_2 \quad , \ 0 < \alpha < 1 \quad (4)$$

The parameter of α, determines the effect of f1 and f2 in the Formula 4.

The amount of J_m is considered as the best fitness value, where using inner class, and each center should be arranged at the center of the data. This result to a small value for J_m, therefore, by getting J_m smaller in the inner class, we can become nearer to the best possible state, but in the case of the outer class, for getting to the desirable state, we attempt to increase the amount of J_m. In order to calculate the amount of fitness, we should edit the related J_m to the situation of the outer class used for getting the fitness. We should decrease the J_m in the outer class, by multiplying the amount of image pixels by the number 255. This is shown as ß. Therefore fitness formula should be changed as Formula 5.

$$Fitness = \alpha \times f_1 + [(1-\alpha) \times (\beta - f_2)] \quad (5)$$

If all of the data in a chromosome are valid set of data centers, and if the number of data in a chromosome is equal to the number of valid data then J_m is calculated based on aforementioned method, that is acceptable with respect to the fact that the number of valid data in each chromosome is different, as it is different for class centers, the value of J_m chromosomes fitness value is not suitable and proportional to the number of centers in each chromosome. Therefore, the formula should be corrected such that to be useful in comparison of the chromosomes.

By increasing the number of the centers, the distance between each x_i and the nearest center are decreased and, J_m value is reduced. The number of valid chromosomes as centers are few therefore J_m is selected. The minimum value of the data centers according to the image nature is determined automatically. We need adding another parameter in addition to calculating J_m to correct the fitness value according to the changes in the number of the centers. We have assigned a suitable penalty factor to increase the number of the data centers. The y parameter is obtained from the total length of the valid data of the chromosome and added as the penalty factor according to the Formula 6.

$$y = \frac{total\ lengh\ of\ chromosome}{length\ of\ valid\ data\ of\ chromosome} \quad (6)$$

Given the effect of Formula 6, fitness will be defined as Formula 7.

$$Fitness = (\alpha \times f_1 + [(1-\alpha) \times (\beta - f_2)]) \times y \quad (7)$$

2.4. Selection

For producing the mating pool of Chromosomes, the roulette wheel technique is used. The main idea in roulette wheel method is, to give more chance to better chromosomes.

2.5. Crossover

After selection of the parent chromosomes, the next step is crossover. In this step, a new offspring is generated by using the parents and the combination of them (Fig. 4).

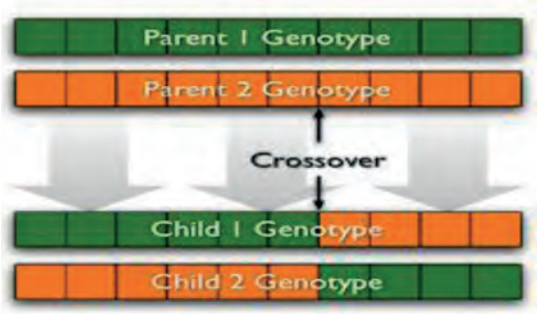

Figure 4. One point crossover operation

2.6. Mutation

Each allele of the chromosomes changes with the value of P_m, that is the probability which mutation will be used for searching in the entire answers interval. The overview of the segmentation process is shown in Fig. 5.

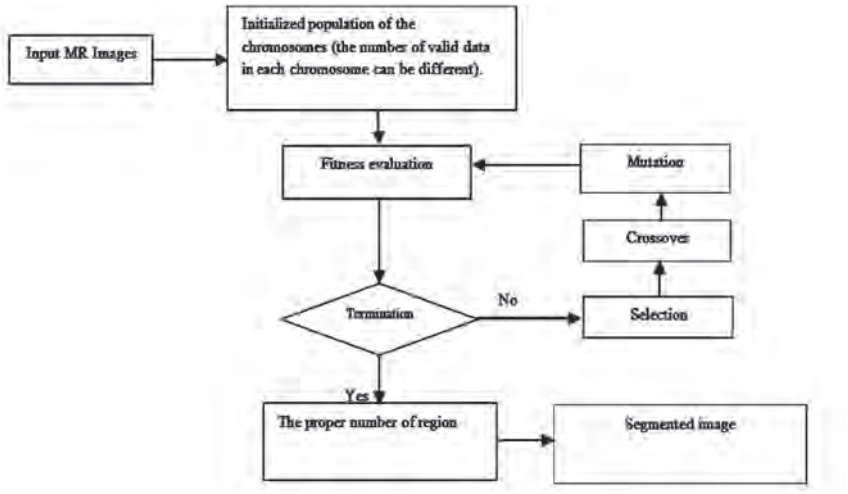

Figure 5. The schematic flow chart of segmentation

3. Results

3.1. Experimental Results with Simulated MR Images

The MR simulated images are downloaded from Brain Web Simulated Brain Database and the algorithms is tested with the Matlab software. The images with the size of 181×217×181 (X×Y×Z) are simulated T1 modality where, slice thickness is 1 mm and intensity is uniform. The initial population is 20 and the maximum number of generations is 25. From the total population, 40 percent of them are selected in each generation. The selected images are good enough for determining the right number of segments and also the location of the center for each segment.

In Fig. 6 the results of the implementation of the proposed automatic segmentation method on the original MR images is shown.

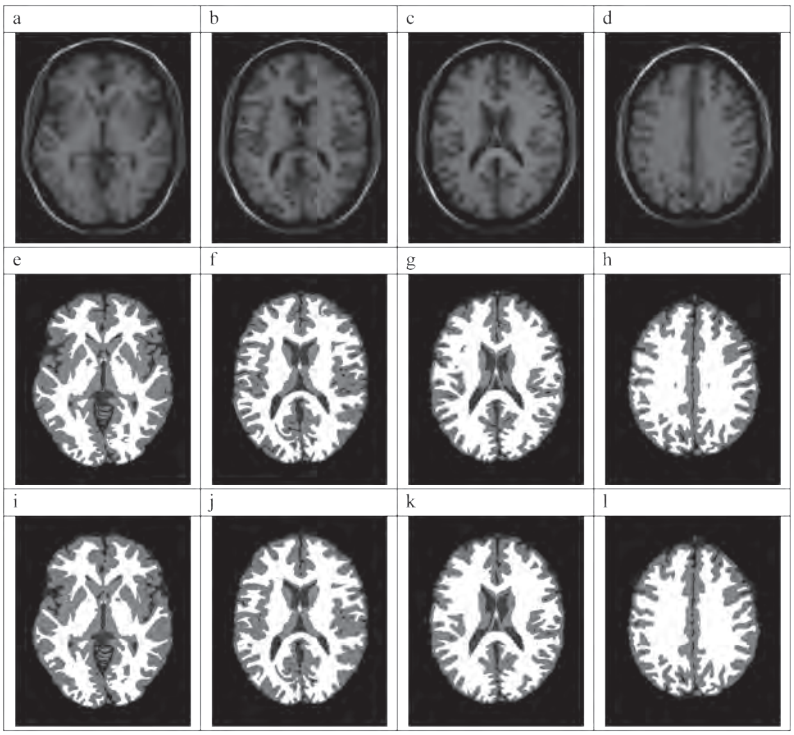

Figure 6. (a), (b), (c) and (d) are the original slices of brain. (e), (f), (g) and (h) are the manual segmentation. (i), (j), (k) and (l) are the segmented images by the proposed method.

The Specificity, Sensitivity, Jaccard and k-index parameters were used to determine the validity of the method. If A and B indicate the results of automatic and manual image segmentation methods, then T_p=B∩A , Fp=A-B , F_n=B-A respectively represent the true-positive, false-positive, and false-negative values .

According to Table 1, the sensitivity [24] is calculated by using Formula 8.

$$Sensitivity = \frac{N_{tp}}{N_{tp} + N_{fn}} \quad (8)$$

The specificity is calculated with Formula 9:

$$Specificity = \frac{N_{tn}}{N_{fp} + N_{tn}} \quad (9)$$

Similarity is equal to Formula (10) [25]:

$$k(A,B) = \frac{2|A \cap B|}{|A+B|} \times 100\% = \frac{2T_p}{|B|+|A|} \times 100\% \quad (10)$$

Jaccard index is equal to Formula (11):

$$j(A,B) = \frac{|A \cap B|}{|A \cup B|} \times 100\% = \frac{T_p}{|T_p| + |F_n| + |F_p|} \times 100\% \quad (11)$$

Table 1. Different modes of voxels

		True class	
		Abnormal	Normal
Detected class	**Abnormal**	N_{tp}	N_{fp}
	Normal	Nf_n	N_{tn}

The parameters set of the genetic operations are determined as shown in Table 2.

Table 2. Parameters for genetic operations

Representation	Bit representation
Crossover type	One point crossover
Crossover rate	0.4
Mutation type	Bit mutation
Mutation rate	0.1

In Table 3, the performance of the proposed method is shown.

Table 3. Results obtained from the proposed method

Initial number of chromosome length	Specificity	Sensitivity	Number of final center	k index	Jaccard similarity
5	0.994	0.965	0.961	0.969	3
5	0.987	0.972	0.953	0.963	3
5	0.974	0.988	0.947	0.957	3
5	0.995	0.959	0.939	0.955	3
5	0.988	0.978	0.949	0.959	3
6	0.996	0.987	0.966	0.976	3
6	0.979	0.982	0.962	0.968	3
6	0.993	0.981	0.960	0.975	3
6	0.996	0.988	0.963	0.977	3

Table 3 shows, when we increase the length of the chromosomes, more accurate answers are mostly obtained.

The results of the presented method on the noisy images are given in Table 4.

Table 4. Results obtained from the proposed method

Initial number of chromosome length	Sensitivity	Specificity	Jaccard similarity	k index	Number of final center
5	0.989	0.972	0.959	0.960	3
5	0.981	0.973	0.952	0.957	3
5	0.971	0.983	0.943	0.956	3
5	0.984	0.967	0.933	0.950	3
5	0.979	0.971	0.942	0.952	3
6	0.987	0.977	0.961	0.948	3
6	0.981	0.983	0.953	0.957	3
6	0.982	0.980	0.955	0.963	3
6	0.989	0.984	0.959	0.971	3

We review the performance of the proposed method in a 3D image with 3% added noise (Fig. 7).

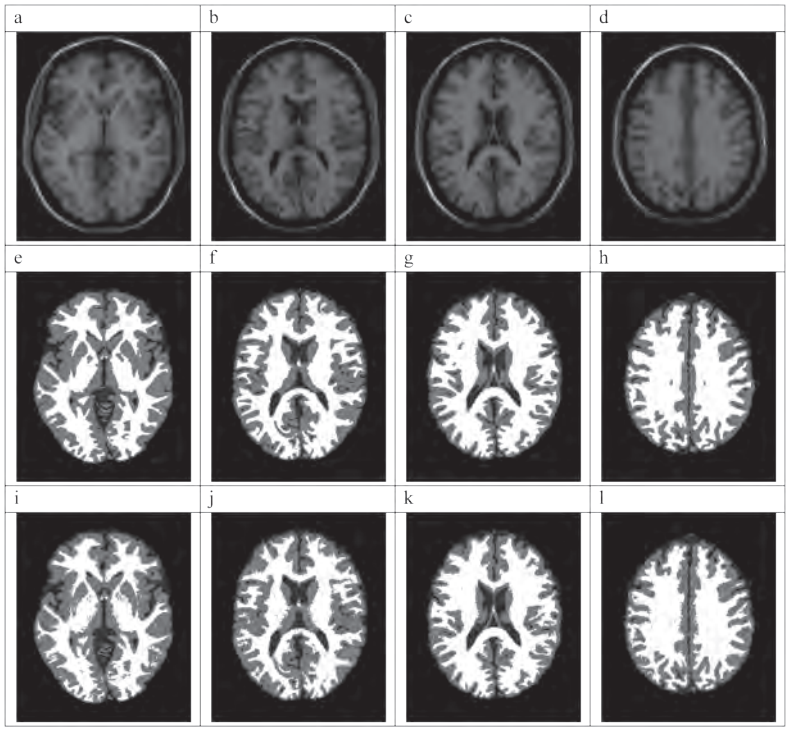

Figure 7. (a), (b), (c), and (d) are the original slices of the brain with 3% noise and 20% intensity of non uniformity. (e), (f), (g), and (h) are the manual segmentation. (i), (j), (k), and (l) are the segmented images by the proposed method with use of three neighbors for each voxels.

We also review the performance of the proposed method in a 3D image with 9% of added noise (Fig. 8).

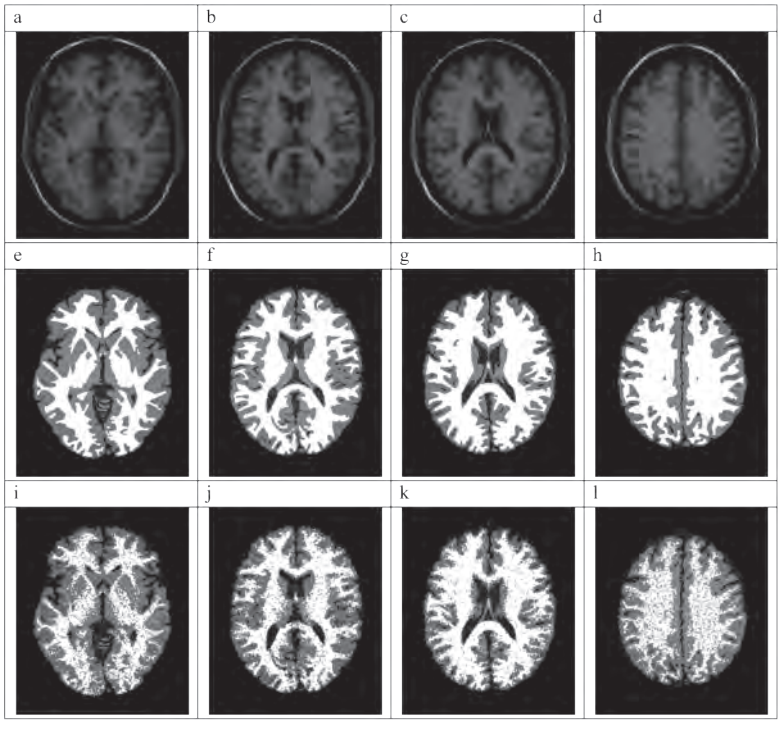

Figure 8. (a), (b), (c), and (d) are the original slices of brain with 9% noise and 20% intensity of non uniformity. (e), (f), (g), and (h) are the manual segmentation. (i), (j), (k), and (l) are the images that are segmented by the proposed method with use of five global neighbors for each voxels.

The misclassification rate (MCR) for average of ten runs of proposed algorithm is listed in Table 5.

Table 5. The misclassification rate of the tissues in simulated MR images data set with different noise levels.

Noise level	Tissue type	MCR for different methods			
		K-means (%)	FCM (%)	EM (%)	Our method (%)
1%	CSF	1.55	2.10	4.99	0.07
	GM	3.25	3.05	0.12	0.11
	WM	2.25	2.02	7.57	0.13
3%	CSF	2.20	2.87	5.53	0.11
	GM	4.78	4.52	1.21	0.14
	WM	2.96	2.71	8.53	0.17
5%	CSF	3.88	4.24	5.49	0.10
	GM	7.07	7.09	4.30	022
	WM	5.04	4.41	7.26	0.31
7%	CSF	7.06	7.00	6.76	0.11
	GM	10.81	10.89	8.55	0.26
	WM	8.42	7.90	8.93	0.37
9%	CSF	10.93	10.52	8.10	0.13
	GM	16.22	16.20	11.17	0.31
	WM	14.74	14.44	17.17	0.44

The genetic algorithm is applied for three chromosomes of length 5, 7, and 9 and the accuracy with different noise levels are compared, the results after 25 iterations are shown in Fig. 9.

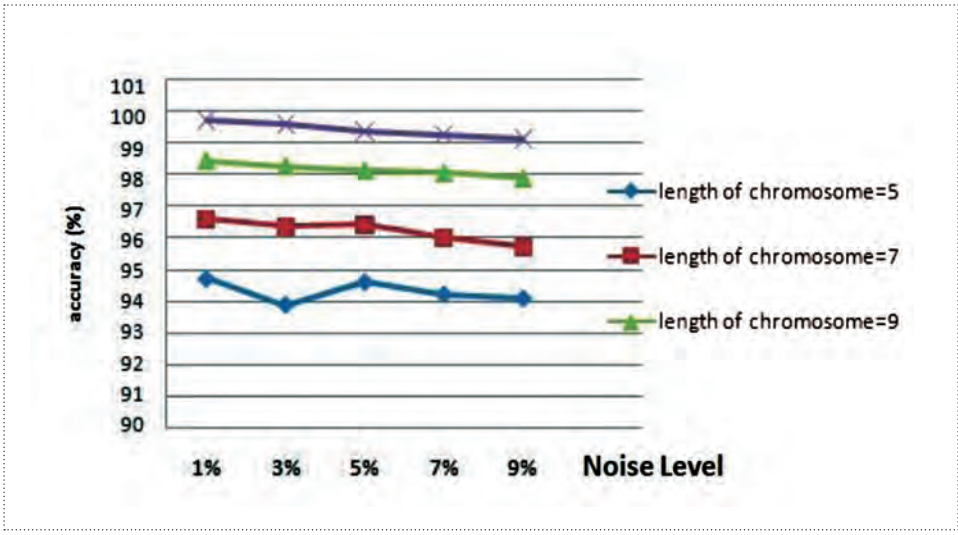

Figure 9. The comparison of noise levels and accuracy, after 25 iteration

3.2. Experimental Results with Real MR Images

The presented algorithm is also implemented on real MR images. Real MR images of 10 patient taken from Imam khomeini hospital (The volume dimension is 256×256×25 and the voxel size is 0.97*0.97*4 mm3). Fig. 10 shows the results of the implementation of the proposed method on the real MR images.

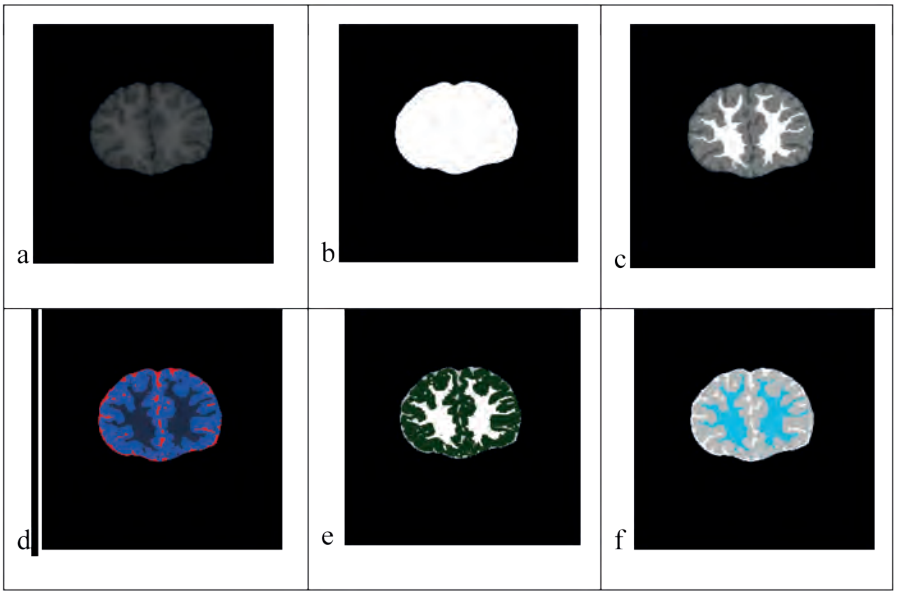

Figure 10. (a) is T1-weighted real MRI image (z=2), b is the background of the image removed from the brain, c is the manual segmentation. (d), (e), and (f) are the images that segmented by the proposed method with use of two, three and four global neighbors for each voxels.

As we can see, only with use of four neighbors for each voxels, the image segmentation is improved.

The quantitative comparison of the accuracy of proposed method with FCM_AWA, SHFCM, MFGFCM, segmentation results is listed in Table 6.

Table 6. Segmentation accuracy of the FCM_AWA, SHFCM, MFGFCM and proposed method in brain MR images.

Noise level	Segmentation accuracy for different methods (Jaccard similarity)			
	FCM_AWA (%)	SHFCM (%)	MFGFCM (%)	Our method (%)
3%	88.29	83.91	88.81	93.13
5%	87.15	83.37	88.67	91.37
9%	81.12	83.11	86.62	89.18

4. Discussion

The quantitative results from simulated and real images with different levels of noise for different algorithms are provided in Tables 5 and Table6. With selecting some of the neighbors in the noisy images, the effect of noise is reduced and the accuracy of segmentation is increased. In Fig. 8, it has been shown that, by implementing a good method we can find better neighbors, and also by using suitable method for adjustment of the voxel weight, we can achieve to an acceptable result only in 25 iterations. As shown in Table 3 and Table4, without interference of human the correct number of segments are automatically discovered.

5. Conclusion

The FCM method suffers from noise detection in the images, but it has been widely used in medical image segmentation. Many researches are done based on FCM algorithms, but none of them are flawless. In this article a new approach to genetic algorithm based on FCM method is presented, the local and non-local neighbors and also inner and outer class data distances are used. We have tested our algorithm with using simulated and real MR images. In the proposed method the effect of noise is decreased and the right numbers of segments are discovered automatically. In the proposed technique the number of genetic iterations is reduced and the convergence speed is increased. Instead of checking all of the neighbors for each voxel, only part of the neighbors are selected which is resulted to a noticeable improvement in the segmentation.

References

[1] S. Witoszynskyj, A. Rauscher, J. R. Reichenbach, and M. Barth, "Phase unwrapping of MR images using ΦUN–A fast and robust region growing algorithm," Medical image analysis, vol. 13, pp. 257-268, 2009.

[2] T.-C. Su, M.-D. Yang, T.-C. Wu, and J.-Y. Lin, "Morphological segmentation based on edge detection for sewer pipe defects on CCTV images," Expert Systems with Applications, vol. 38, pp. 13094-13114, 2011.

[3] L. Gupta, U. G. Mangai, and S. Das, "Integrating region and edge information for texture segmentation using a modified constraint satisfaction neural network," Image and Vision Computing, vol. 26, pp. 1106-1117, 2008.

[4] D. N. Chun and H. S. Yang, "Robust image segmentation using genetic algorithm with a fuzzy measure," Pattern recognition, vol. 29, pp. 1195-1211, 1996.

[5] R. A. Heckemann, J. V. Hajnal, P. Aljabar, D. Rueckert, and A. Hammers, "Automatic anatomical brain MRI segmentation combining label propagation and decision fusion," NeuroImage, vol. 33, pp. 115-126, 2006.

[6] M. Cabezas, A. Oliver, X. Lladó, J. Freixenet, and M. Bach Cuadra, "A review of atlas-based segmentation for magnetic resonance brain images," Computer methods and programs in biomedicine, vol. 104, pp. e158-e177, 2011.

[7] Z. Ji, Y. Xia, Q. Chen, Q. Sun, D. Xia, and D. D. Feng, "Fuzzy c-means clustering with weighted image patch for image segmentation," Applied Soft Computing, vol. 12, pp. 1659-1667, 2012.

[8] Z. M. Wang, Y. C. Soh, Q. Song, and K. Sim, "Adaptive spatial information-theoretic clustering for image segmentation," Pattern Recognition, vol. 42, pp. 2029-2044, 2009.

[9] S. Kannan, S. Ramathilagam, R. Devi, and E. Hines, "Strong fuzzy c-means in medical image data analysis," Journal of Systems and Software, vol. 85, pp. 2425-2438, 2012.

[10] S. Kannan, S. Ramathilagam, R. Devi, and A. Sathya, "Robust kernel FCM in segmentation of breast medical images," Expert Systems with Applications, vol. 38, pp. 4382-4389, 2011.

[11] S. Kannan, A. Sathya, S. Ramathilagam, and R. Devi, "Novel segmentation algorithm in segmenting medical images," Journal of Systems and Software, vol. 83, pp. 2487-2495, 2010.

[12] B. Caldairou, N. Passat, P. A. Habas, C. Studholme, and F. Rousseau, "A non-local fuzzy segmentation method: application to brain MRI," Pattern Recognition, vol. 44, pp. 1916-1927, 2011.

[13] Y. He, M. Yousuff Hussaini, J. Ma, B. Shafei, and G. Steidl, "A new fuzzy c-means method with total variation regularization for segmentation of images with noisy and incomplete data," Pattern Recognition, vol. 45, pp. 3463-3471, 2012.

[14] Z.-X. Ji, Q.-S. Sun, and D.-S. Xia, "A modified possibilistic fuzzy< i> c</i>-means clustering algorithm for bias field estimation and segmentation of brain MR image," Computerized Medical Imaging and Graphics, vol. 35, pp. 383-397, 2011.

[15] Z.-X. Ji, Q.-S. Sun, and D.-S. Xia, "A framework with modified fast FCM for brain MR images segmentation," Pattern Recognition, vol. 44, pp. 999-1013, 2011.

[16] Z. Ji, Q. Sun, Y. Xia, Q. Chen, D. Xia, and D. Feng, "Generalized rough fuzzy c-means algorithm for brain MR image segmentation," Computer methods and programs in biomedicine, vol. 108, pp. 644-655, 2012.

[17] J. Wang, J. Kong, Y. Lu, M. Qi, and B. Zhang, "A modified FCM algorithm for MRI brain image segmentation using both local and non-local spatial constraints," Computerized Medical Imaging and Graphics, vol. 32, pp. 685-698, 2008.

[18] K. Sikka, N. Sinha, P. K. Singh, and A. K. Mishra, "A fully automated algorithm under modified FCM framework for improved brain MR image segmentation," Magnetic Resonance Imaging, vol. 27, pp. 994-1004, 2009.

[19] C.-C. Lai and C.-Y. Chang, "A hierarchical evolutionary algorithm for automatic medical image segmentation," Expert Systems with Applications, vol. 36, pp. 248-259, 2009.

[20] J.-Y. Yeh and J. Fu, "A hierarchical genetic algorithm for segmentation of multi-spectral human-brain MRI," Expert Systems with Applications, vol. 34, pp. 1285-1295, 2008.

[21] J. Fu, C. Chen, J. Chai, S. T. Wong, and I. Li, "Image segmentation by EM-based adaptive pulse coupled neural networks in brain magnetic resonance imaging," Computerized Medical Imaging and Graphics, vol. 34, pp. 308-320, 2010.

[22] W.-B. Tao, J.-W. Tian, and J. Liu, "Image segmentation by three-level thresholding based on maximum fuzzy entropy and genetic algorithm," Pattern Recognition Letters, vol. 24, pp. 3069-3078, 2003.

[23] M. Chen, A. Carass, J. Oh, G. Nair, D. L. Pham, D. S. Reich, et al., "Automatic magnetic resonance spinal cord segmentation with topology constraints for variable fields of view," NeuroImage, vol. 83, pp. 1051-1062, 2013.

[24] A. R. Van Erkel and P. M. T. Pattynama, "Receiver operating characteristic (ROC) analysis: basic principles and applications in radiology," European Journal of radiology, vol. 27, pp. 88-94, 1998.

[25] J. K. Udupa, V. R. Leblanc, Y. Zhuge, C. Imielinska, H. Schmidt, L. M. Currie, et al., "A framework for evaluating image segmentation a